

MASTER OF SCIENCE THESIS

Geometric Control of a Quadrotor with a Suspended Load

Subtitle

N.N. Vo

June 20, 2017



Geometric Control of a Quadrotor with a Suspended Load

Subtitle

MASTER OF SCIENCE THESIS

For obtaining the degree of Master of Science in Mechanical
Engineering at Delft University of Technology

N.N. Vo

June 20, 2017

The work in Master of Science Thesis was supported by Alten. Their cooperation is hereby gratefully acknowledged.



Delft University of Technology

Copyright © Delft Center for Systems and Control
All rights reserved.

DELFT UNIVERSITY OF TECHNOLOGY
DELFT CENTER FOR SYSTEMS AND CONTROL

The undersigned hereby certify that they have read and recommend to the Faculty of Mechanical, Maritime and Materials Engineering for acceptance a thesis entitled “**Geometric Control of a Quadrotor with a Suspended Load**” by **N.N. Vo** in partial fulfillment of the requirements for the degree of **Master of Science**.

Dated: June 20, 2017

Supervisor:

dr.ir. T. Keviczky

Readers:

ir. B. van Vliet

Abstract

A Quadrotor is a type of Unmanned Aerial Vehicle that has received an increasing amount of attention recently with many applications including search and rescue, surveillance, supply of food and medicines as disaster relief and object manipulation in construction and transportation.

An interesting subproblem is the control of the position of a cable suspended load. The challenge is in the fact that the Quadrotor-Load system is highly nonlinear and under-actuated. The load cannot be controlled directly and has a natural swing at the end of each Quadrotor movement.

This thesis presents a Nonlinear Geometric Control approach for the position tracking of a cable suspended load. Geometric Control applies differential geometric techniques to systems modeling and control. The Quadrotor-Load system dynamics are modeled on so called manifolds, smooth nonlinear configuration geometric spaces. Analyzing these geometric structures with the principles of differential geometry allows the system to be modeled in an unambiguous coordinate-free dynamic fashion, while avoiding the problem of singularities that would occur on local charts.

A Nonlinear Geometric Control design is based on the geometric properties of the system. A backstepping approach allows different controller to control different flight modes, which are accountable for the Quadrotor attitude, Load attitude and Load position, in a cascaded structure.

Different cases are tested to investigate the possibilities and limitations of Nonlinear Geometric Control. A Linear Quadratic Regulator is derived to compare control performance. Simulations of both the linear and nonlinear controller are presented. Results show that....

Acknowledgements

I would like to thank my supervisors dr.ir. T. Keviczky from Delft Center of Systems and Control, and ir. B. van Vliet from Alten Nederland B.V. for their assistance during my research and the writing of this thesis. I would also like to thank all colleagues from Alten and TU Delft for their time and advices.

Delft, University of Technology
June 20, 2017

N.N. Vo

Table of Contents

Abstract	v
Acknowledgements	vii
1 Introduction	1
1-1 Aim and Motivation	3
1-2 Organization of the Report	4
2 Dynamic Model	5
2-1 Modeling Assumptions	5
2-2 Geometric Mechanics	8
2-3 Quadrotor-Load Model	10
2-4 Classical Modeling	13
2-5 Stability Analysis	14
2-6 Summary	14
3 Geometric Control Design	17
3-1 Backstepping Control	17
3-2 Configuration Errors	18
3-3 Quadrotor Attitude Tracking	20
3-4 Load Attitude Tracking	21
3-5 Load Position Tracking	21
3-6 Parameter- and State Estimation	22
3-7 Summary	22

4	Experiments and Results	25
4-1	Setup	25
4-1-1	Command Filtering	27
4-2	Experiments	28
4-2-1	Performance Criteria	28
4-2-2	Case A	29
4-2-3	Case B	29
4-2-4	Case C	29
4-3	Results	30
4-3-1	Case A	30
4-3-2	Case B	31
4-3-3	Case C	32
4-4	Conclusion	33
5	Conclusions and Future Work	35
5-1	Summary and Conclusions	35
5-2	Recommendations for Future Work	35
5-2-1	Investigate Implementation	35
5-2-2	Modeling Constraints	36
5-2-3	Hybrid Modeling	36
5-2-4	Trajectory Generation	36
	Minimum Snap Trajectory Generation	36
A	Appendix	37
A-1	Derivation of Equations of motion	37
A-1-1	Load Dynamics	37
A-2	LQR controller	37
A-2-1	Modeling	37
A-2-2	Controller	39
A-3	Figures	40
A-4	MATLAB code	40
A-4-1	A MATLABListing	41
	Bibliography	45
	Acronyms	48

List of Figures

2-1	Quadrotor model representation	6
2-2	Quadrotor with Load model representation	6
2-3	Configuration Space of a 2-link arm	8
2-4	A manifold locally resembles a Euclidean space	9
2-5	9
2-6	Quadrotor-Load model representation	10
2-7	Quadrotor-Load model representation	13
2-8	14
3-1	Backstepping Control representation of the QR	18
3-2	Backstepping Control representation of the QR-Load system	18
3-3	Quadrotor Attitude Controller	20
3-4	21
3-5	21
4-1	LQR control design	26
4-2	Representation of the command filter	28
4-3	Desired Load Position Case A	29
4-4	Desired Load Position Case B	29
4-5	Desired Load Position Case C	29
4-6	Results Nonlinear Geometric Control Case A	30
4-7	Results Nonlinear Geometric Control Case B	31
4-8	Results Nonlinear Geometric Control Case C	32
A-1	Simulink Command Filter	40

List of Tables

2-1	Modeling assumptions	7
4-1	Modeling Parameters	25
4-2	Controller Gains	27

Chapter 1

Introduction

A Quadrotor (QR) is a type of Unmanned Aerial Vehicle (UAV) that has received an increasing amount of attention recently with many applications being actively investigated. Possible applications include search and rescue, surveillance, reliable supply of food and medicines as disaster relief and object manipulation in construction and transportation. It has already proven itself useful for many tasks like multi-agent missions, mapping, explorations, transportation and entertainment such as acrobatic performances.

The inspiration for this research is build upon the idea of creating a system of multiple autonomous QRs for a cooperative towing task. The advantage of such a system for object manipulation is the possibility to reduce complexity of the individual robot, decrease cost over traditional robotic systems and high reliability. One can think of examples in nature, where individuals coordinate, cooperate and collaborate to perform tasks that they individually can not accomplish. Redundancy makes development of fail safe control methods possible and can extend the capabilities of a single robot.

Bart: suggestion: creating a system of multiple autonomous QRs?

Nam: Zin aangepast.

Considering a multi-agent task, one can think of multiple QRs assisting in the transportation of a common load. This cooperation can be executed in many ways, but this research focuses on QRs with a cable-suspended load in motion. The suspended object naturally continues to swing at the end of every movement. In case a residual motion can result in damage or in order to avoid obstacles and path following, an accurate positioning is required. Reducing the oscillation, or controlling the position of the suspended load might be necessary, but is challenging in the fact that this cable-suspended system is under-actuated. Possible objectives are minimizing the oscillations of the load during or after motion, minimizing the time to position the load, trajectory tracking, trajectory generation and obstacle avoidance.

Bart: Suggestion place under motivation of research inspiration, this forms a nice bridge.

Nam: Ik heb dit juist naar boven geplaatst. The inspiration single robot.

1-1 Aim and Motivation

The aim is to control the position of a suspended load using a QR. Before considering multiple QRs, it is important to investigate the possibilities of a single QR system. Hence, in this research a single QR is considered for the transportation of a cable suspended load, which will exert additional forces and torques on the QR. This is a challenging control problem in the fact that the QR system is under-actuated. Adding a suspended load will add extra DOFs and oscillations of the load occur at the end of every movement.

Bart: Suggestion: Since QRs with suspended load are scarcely investigated it is important to investigate a single QR first before the multiple QRs can be considered.

Nam: Zie boven

The system can be divided into two subsystems. The first subsystem is where the cable tension is non-zero and the distance between the QR and the load is defined by the cable length. Both QR and load are coupled as one system. The second subsystem is where the cable tension is zero, such that the QR and load in free fall are two separate decoupled systems. This research focuses on the first subsystem, such that the cable tension is non-zero. In order to control both subsystems, hybrid control must be applied, which is considered out of the scope of this research.

Former work on QR attitude- and position control often rely on linear control methods such as PID controller[?], MPC [1] and LQR control [?]. The dynamics are linearized around an equilibrium point, describing the system dynamics by a set of linear differential equations. The control of a QR-Load system is a very specific case, and former work includes MPC [2] and LQR[?] control approaches, where an optimal control strategy is used to minimize the swing of the load.

The reason that linear control near an equilibrium state is commonly applied, is partly to avoid difficulties that come with modeling and controlling the non-linearities of the system. Non-linear control systems are often governed by nonlinear differential equations and are able to represent the dynamics in a more realistic manner. However, linear control limits the system to small angle movements, as the optimization will not allow large angles that deviate too far from the linearized point. For applications that require fast aggressive maneuvers, this type of modeling and control will not be sufficient.

A possible nonlinear control approach is Nonlinear MPC, which is a variant of MPC that uses a nonlinear dynamical system to predict the required inputs. While these problems are convex in linear MPC, in nonlinear MPC they are not convex anymore. This poses challenges for both Nonlinear MPC stability theory and numerical solution.

Nonlinear Geometric Control is a nonlinear model based control technique based on a modeling approach involving the concepts of differential geometry. This results in a globally defined coordinate-free dynamical model, while preventing issues regarding singularities, and enabling the design of controllers that offer almost-global convergence properties.

Former work includes a nonlinear geometric control of a QR [3, 4] and nonlinear geometric control of the load position, load attitude and QR attitude of a QR-Load system [5, 6,

7]. Geometric Control for the control of QR systems is used less frequently, despite the advantageous properties of differential geometry.

This motivates to investigate the possibilities and limitations of the less used nonlinear Geometric Control design, and compare this to a commonly used linear control strategy. The question is which advantages or disadvantages this nonlinear approach has compared to a linear approach, in terms of stability and performance.

Different aspects involving the modeling and control for the QR-Load system must be investigated, for it can be expected that the non-linearity will have a great influence in the representation of the dynamics and the stability, accuracy and type of control design.

System consists of two sub-systems Limited to subsystem where the tension of the cable is non-zero.

1-2 Organization of the Report

In this first chapter, a brief introduction of the subject is given and the problem is described. This is followed by discussing the aim, motivation and contributions of this thesis for this research. The organization of the report is as follows.

In Chapter 2 the dynamics of the QR-Load system is described by the laws of kinematics and the application of Newton's laws or Lagrangian mechanics. Opposed to the classical modeling techniques, it is also possible to describe the system's configuration space as a differentiable manifold using the tools of differential geometry. Geometric Mechanics is used to understand and derive the equations of motion of a system in order to allow its analysis and design.

The system dynamics are represented on nonlinear manifolds and this allows nonlinear geometric controllers to be designed on these same manifolds. The control design is presented in Chapter 3. The controller has a cascaded structure, where the different control loops are accountable for different flight modes.

Different tracking objectives can be defined in order to test the performance of both an LQR control design and a nonlinear Geometric Control design. Chapter 4 describes the experiments that are done to investigate the abilities and performance of a nonlinear Geometric Control design. The results and findings are presented and discussed.

In the final chapter a summary of the thesis is given, followed by the conclusions that were made based on the results of the experiments. Finally, recommendations are given which could serve as an starting point for future work.

Chapter 2

Dynamic Model

In Section 2-3 the model dynamics of the QR-Load system are obtained by describing the dynamics on nonlinear manifolds, with the concepts of differential geometry.

A mathematical model of the system needs to be derived in order to simulate and study the effects of Geometric Control. The assumptions that are applied to simplify the model are discussed in Section 2-1.

In Section 2-2 an introduction is given about Geometric Mechanics, which is a modern description of the classical mechanics from the perspective of Differential Geometry. Differential Geometry is a discipline in mathematics that studies manifolds and their geometric properties, using the tools of calculus. Geometric Mechanics is used to model the QR-Load system, which is described in Section 2-3.

To derive the equations of motions traditional modeling methods often parameterize the rotations in a local coordinate system. Euler angles are commonly used, however these coordinates might result in singularities. Furthermore, there are 24 possible sets of Euler angles and many different conventions are used, which leads to ambiguity. The definition of Euler angles is not unique and a sequence of rotations is not commutative. Therefore, Euler angles are never expressed in terms of the external frame, or in terms of the co-moving rotated body frame, but in a mixture.

In order to avoid these complexities, the dynamics of the QR-Load system can be globally expressed on the Special Orthogonal Group $SO(3)$, 2-sphere S^2 and Special Euclidean Group $SE(3)$. This leads to a compact notation of the equations of motion, making the large amount of trigonometric functions unnecessary, that Euler angles normally introduce.

2-1 Modeling Assumptions

The QR model representation is shown in Figure 2-1. Three Cartesian coordinate frames are defined:

- The body-fixed reference frame $\{\mathcal{B}\}$ (Body Frame)
with unit vectors $\{\mathbf{b}_1, \mathbf{b}_2, \mathbf{b}_3\}$ along the axes

- The ground-fixed reference frame $\{\mathcal{I}\}$ (Inertial Frame)
with unit vectors $\{\mathbf{e}_1, \mathbf{e}_2, \mathbf{e}_3\}$ along the axes
- The intermediary frame $\{\mathcal{C}\}$, ($\{\mathcal{I}\}$ rotated by the yaw angle ψ)
with unit vectors $\{\mathbf{c}_1, \mathbf{c}_2, \mathbf{c}_3\}$ along the axes



Figure 2-1: Quadrotor model representation



Figure 2-2: Quadrotor with Load model representation

The position of the body frame is described by a vector evolving on \mathbb{R}^3 , and is represented with respect to the inertial frame. The orientation, also called attitude, of the body frame with respect to the inertial frame evolves on a nonlinear space, for which several methods exist to describe this, such as *Euler Angles*, quaternions or rotation matrices.

The complex dynamics of the rotors and their interactions with drag and thrust forces are represented by a simplified model. The angular speed ω_i of rotor i , for $i = 1, \dots, 4$, generates a force F_i parallel to the direction of the rotor axis of rotor i , given by

$$F_i = \left(\frac{K_v K_\tau \sqrt{2\rho A}}{K_t} \omega_i \right)^2 = b\omega_i^2 \quad (2-1)$$

where K_v, K_t are constants related to the motor properties, ρ is the density of the surrounding air, A is the area swept out by the rotor, K_τ is a constant determined by the blade configuration and parameters, and b is the thrust factor.

The torque around the axis of rotor i , for $i = 1, \dots, 4$, generated due to drag is given by

$$M_i = \frac{1}{2} R \rho C_D A (\omega_i R)^2 = d\omega_i^2 \quad (2-2)$$

where R is the radius of the propeller, C_D is a dimensionless constant, and d is the drag constant.

For given desired total thrust f and total moment $M = [M_\phi \ M_\theta \ M_\psi]^T$, the required rotor speeds can be calculated by solving the following equation

$$\begin{bmatrix} f \\ M_\phi \\ M_\theta \\ M_\psi \end{bmatrix} = \begin{bmatrix} b & b & b & b \\ 0 & -lb & 0 & lb \\ lb & 0 & -lb & 0 \\ -d & d & -d & d \end{bmatrix} \begin{bmatrix} \omega_1^2 \\ \omega_2^2 \\ \omega_3^2 \\ \omega_4^2 \end{bmatrix} \quad (2-3)$$

where l is the distance from the rotor to the QR's CoM and M_ϕ, M_θ, M_ψ denote the moments around the x, y, z -axis in $\{\mathcal{B}\}$, resp.

Table 2-1 shows the most common assumptions that are used for modeling the QR, simplifying the complexity of the model.

Bart: Refer to table 2-2?

Nam: Wat bedoel je?

Modeling assumptions Quadrotor model

- The structure of the QR is rigid and symmetric.
Elastic deformations and shock (sudden accelerations) of the QR are ignored.
- The mass distribution of the QR is symmetrical in the x-y plane.
- The inertia matrix is time-invariant.
- Aerodynamic effects acting on the QR are neglected.
Blade flapping, Turbulence, Ground Effects.
- The air density around the QR is constant.
- The propellers are rigid \Rightarrow The thrust produced by rotor i is parallel to the axis of rotor i .
- Drag factor d and thrust factor b are approximated by a constant.
Thrust force F_i and moment M_i of each propeller is proportional to the square of the propeller speed.

Modeling assumptions Quadrotor-Load model

- The cable is modeled as a rigid and massless cable.
- The cable is connected to a friction-less joint at the origin of the body-fixed.
- The tension in the cable is considered to be non-zero.
This implies that the QR-Load subsystem, consisting of a separate QR and Load in free fall, is disregarded.
- Aerodynamic effects acting on the load are neglected.
reference frame.
- Assumption
Details Assumption 2

Table 2-1: Modeling assumptions

2-2 Geometric Mechanics

In Geometric Mechanics the configuration space of systems is a *group manifold* instead of a Euclidean space. The kinetic and potential energies are expressed in terms of this configuration space and their tangent spaces. It explores the geometric structure of a Lagrangian- or Hamiltonian system through the concepts of vector calculus, linear algebra, differential geometry, and non-linear control theory. Geometric mechanics provides fundamental insights into the nonlinear system mechanics and yields useful tools for dynamics and control theory.

Euler angles are kinematically singular since the transformation from their time rates of change to the angular velocity vector is not globally defined. Furthermore, when angular errors are large, the difference in Euler angles is no longer a good metric to define the orientation error. Local coordinates often require symbolic computational tools due to complexity of multi-body systems. Hence, the error is rather written as the required rotation to get from the current to a desired orientation. As a result, the equations of motion and the control systems can be developed on a configuration manifold in a coordinate-free, compact, unambiguous manner, while singularities of local parameterization are avoided.

To illustrate the difference in configuration spaces, an example is given of a 2-link arm, where the configuration can be expressed by 2 coordinates, see in Figure 2-3. Figure 2-3b represents the configuration space as a Cartesian space, where the same dots represent one of the many identical configurations. This shows that this representation suffers from singularities caused by multiple points in one representation being mapped onto a single point in another representation. Figure 2-3c shows the configuration space as a geometric shape called a *torus*, a manifold where every configuration is mapped uniquely.

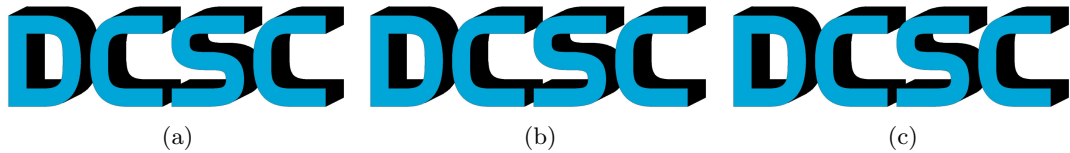


Figure 2-3: Configuration Space of a 2-link arm

Manifolds The fundamental object of differential geometry a manifold. A manifold is a mathematical space, a collection of points, that locally resembles Euclidean space near each point. Examples are a plane, a ball, a torus and a sphere. Manifolds are important objects in mathematics and physics because they allow more complicated structures to be expressed and understood in terms of the relatively well-understood properties of simpler spaces. In Figure 2-4 is illustrated that each point of an n -dimensional manifold has a neighborhood that is homeomorphic to the n -dimensional Euclidean space, meaning that there is a continuous function describing the relation between these spaces.

A differentiable manifold is a smooth and continuous manifold and is locally similar enough to a linear space to allow to do calculus. One can define directions, tangent spaces, and differentiable functions on such a manifold. Each point of an n -dimensional differentiable manifold has a tangent space, which is an n -dimensional Euclidean space consisting of the



Figure 2-4: A manifold locally resembles a Euclidean space

tangent vectors of the curves that pass through that point. In Figure 2-5a the manifold \mathbb{S}^2 represents as a sphere, with a tangent space at point x , denoted by $T_x\mathbb{S}^2$. Taking the derivative at a point on a manifold is equivalent to a tangent vector at that point. Meaning that derivatives are conceptually equivalent to an infinitesimally short tangent vector.



(a) Representation of a manifold with a tangent space

(b) Identity map of $SO(3)$ with Lie Algebra $\mathfrak{so}(3)$

Figure 2-5

Configuration Spaces Rotation matrices are used to provide a global representation of the attitude of a rigid body, by mapping a representation of vectors expressed in $\{\mathcal{B}\}$ to a representation expressed in $\{\mathcal{I}\}$ [8, 9]. The configuration of the QR attitude is a rotation matrix R in the Special Orthogonal Group $SO(3)$ defined as

$$SO(3) \triangleq \{R \in \mathbb{R}^{3 \times 3} | RR^T = I_{3 \times 3}, \det(R) = 1\} \quad (2-4)$$

$SO(3)$ is the group of all rotations about the origin of a 3-D Euclidean space, which preserves the origin, Euclidean distance and orientation. Every rotation has a unique inverse rotation and the identity map satisfies the definition of a rotation. The elements of *Lie Algebra* $\mathfrak{so}(3)$, a property associated with $SO(3)$, are the elements of the tangent space of $SO(3)$ at the identity element, see Figure 2-5b. These elements define the relation between the rotation R and its derivative \dot{R} , such that

$$\dot{R} = R\hat{\Omega} \quad (2-5)$$

For $n \in \mathbb{N}$, $\mathfrak{so}(3)$ is the vector space of skew-symmetric matrices in $\mathbb{R}^{n \times n}$ and defined as

$$\mathfrak{so}(n) \triangleq \{S \in \mathbb{R}^{n \times n} | S^T = -S\} \quad (2-6)$$

The linear map $\hat{\cdot} : \mathbb{R}^3 \rightarrow \mathfrak{so}(3)$ is an isomorphism between \mathbb{R}^3 and the set of 3×3 skew symmetric matrices. $\cdot^\vee : \mathfrak{so}(3) \rightarrow \mathbb{R}^3$ denotes the inverse isomorphism. The mapping between the body angular velocity vector $\Omega \in \mathbb{R}^3$ and $\hat{\Omega} \in \mathfrak{so}(3)$ can be written as

$$\hat{\Omega} = \begin{bmatrix} 0 & -\Omega_3 & \Omega_2 \\ \Omega_3 & 0 & -\Omega_1 \\ -\Omega_2 & \Omega_1 & 0 \end{bmatrix}, \quad \begin{bmatrix} 0 & -\Omega_3 & \Omega_2 \\ \Omega_3 & 0 & -\Omega_1 \\ -\Omega_2 & \Omega_1 & 0 \end{bmatrix}^\vee = \Omega \quad (2-7)$$

The configuration space of the load is represented on a 2-sphere, defined as

$$\mathbb{S}^2 \triangleq \{q \in \mathbb{R}^3 | q \cdot q = 1\} \quad (2-8)$$

$$\dot{q} = \omega \times q \quad (2-9)$$

where ω is the angular velocity of the suspended load.

2-3 Quadrotor-Load Model

The Quadrotor-Load model is shown in Figure 2-6, where the unit vector q gives the direction from the QR to the Load expressed in $\{\mathcal{B}\}$. The focus lies on the subsystem where the cable tension is considered to be non-zero. The position of the QR and Load are related by

$$x_Q = x_L - Lq \quad (2-10)$$

where x_Q is the position of the QR's CoM, x_L is the position of the load, and L is the length of the cable.



Figure 2-6: Quadrotor-Load model representation

Dynamics and optimal control problems for rigid bodies are studied in [10], incorporating their geometric features. The focus lies on obtaining geometric properties of the dynamics of rigid bodies, how their configuration can be described and how these geometric properties are utilized in control system analysis and design.

Considering the properties of the system, the QR is described as a rigid body with six degrees of freedom, driven by forces and moments. The configuration of the QR can be described by the location of its CoM and its attitude, which are described in Euclidean space $x_Q \in \mathbb{R}^3$ and in a nonlinear space $R \in SO(3)$, respectively. The configuration of the load can also be described by its location and attitude, described in Euclidean space $x_L \in \mathbb{R}^3$ and on a two-sphere $q \in \mathbb{S}^2$.

To develop the Euler-Lagrange equations for mechanical systems that evolve on a Lie group, an approach developed by [10, 11, 12, 13] is used.

The basic idea is the variations of the curves that are e

This approach is based on Hamilton's principle, which states that the evolution of a physical system is a solution of the functional equation given by

$$\frac{\delta S}{\delta \mathbf{q}(t)} = 0 \quad (2-11)$$

where \mathbf{q} defines the configuration space. S is the action integral, defined as

$$S = \int_{t_1}^{t_2} \mathcal{L} dt \quad (2-12)$$

where $\mathcal{L} = \mathcal{T} - \mathcal{U}$ is the Lagrangian of the system, and \mathcal{T}, \mathcal{U} are the kinetic and potential energy, respectively.

Hamilton's principle of least action states that the path a conservative mechanical system takes between two configurations q_1 and q_2 at time t_1 and t_2 , is the one for which Equation 2-12 is a stationary point, resulting in

$$\delta S = \int_{t_1}^{t_2} \delta \mathcal{L} dt = 0 \quad (2-13)$$

where $\delta \mathcal{L}$ is the variation of the Lagrangian. For systems with non-conservative forces and moments, Equation 2-13 is extended to

$$\delta S = \int_{t_1}^{t_2} (\delta W + \delta \mathcal{L}) dt = 0 \quad (2-14)$$

where δW is the virtual work. Equation 2-14 is applied to the QR-Load system, where the configuration manifold is $\mathbb{R}^3 \times \mathbb{S}^2 \times SO(3)$. With the following states

$$\mathbf{x} = [x_L \quad \dot{x}_L \quad q \quad \omega \quad R \quad \Omega]^T \quad (2-15)$$

Euler-Lagrange Equation 2-13 can be satisfied if the following Euler-Lagrange equation holds

$$\frac{\delta \mathcal{L}}{\delta \mathbf{q}} - \frac{d}{dt} \frac{\delta \mathcal{L}}{\delta \dot{\mathbf{q}}} = 0 \quad (2-16)$$

where the Lagrangian $\mathcal{L} = \mathcal{T} - \mathcal{U}$. The kinetic energy for the system is denoted as

$$\mathcal{T} = \frac{1}{2} m_Q \dot{x}_Q \cdot \dot{x}_Q + \frac{1}{2} m_L \dot{x}_L \cdot \dot{x}_L + \frac{1}{2} \Omega \cdot J \cdot \Omega \quad (2-17)$$

and the potential energy is denoted as

$$\mathcal{U} = m_Q g x_Q \cdot e_3 + m_L g x_L \cdot e_3 \quad (2-18)$$

where g is the gravity constant. The energy can be rewritten in terms of q and x_L , by substituting Equation 2-10, giving

$$\mathcal{T} = \frac{1}{2} (m_Q + m_L) \dot{x}_L \cdot \dot{x}_L - m_Q L \dot{x}_L \cdot \dot{q} + \frac{1}{2} m_Q L^2 \dot{q} \cdot \dot{q} + \frac{1}{2} \Omega \cdot J \cdot \Omega \quad (2-19)$$

$$\mathcal{U} = (m_Q + m_L) g x_L \cdot e_3 - m_Q g L q \cdot e_3 \quad (2-20)$$

The variations of the \mathcal{T} and \mathcal{U} are approximated by a first-order Taylor approximation, which results in

$$\begin{aligned} \delta \mathcal{T} &\approx \frac{\partial \mathcal{T}}{\partial \dot{x}_L} \delta \dot{x}_L + \frac{\partial \mathcal{T}}{\partial \dot{q}} \delta \dot{q} + \frac{\partial \mathcal{T}}{\partial \Omega} \delta \Omega \\ &= ((m_Q + m_L) \dot{x}_L - m_Q L \dot{q}) \cdot \delta \dot{x}_L + (-m_Q L \dot{x}_L + m_Q L^2 \dot{q}) \cdot \delta \dot{q} + J \Omega \cdot \delta \Omega \end{aligned} \quad (2-21)$$

$$\begin{aligned}
\delta\mathcal{U} &\approx \frac{\partial\mathcal{U}}{\partial x_L}\delta x_L + \frac{\partial\mathcal{U}}{\partial q}\delta q \\
&= (m_Q + m_L)ge_3 \cdot \delta x_L - m_QgL e_3 \cdot \delta q
\end{aligned} \tag{2-22}$$

The first term of virtual work is obtained from f acting on the **QR** and is given by the following term,

$$\begin{aligned}
\delta W_1 &= fRe_3 \cdot \sum_{j=1}^3 \frac{\partial x_Q}{\partial \mathbf{q}_j} \delta \mathbf{q}_j \\
&= fRe_3 \cdot (\delta x_L - L\delta q)
\end{aligned} \tag{2-23}$$

where $\mathbf{q}_j = x_L, q, R$ and x_Q is substituted by Equation 2-10 The second term of virtual work is obtained from M acting on the **QR**. This gives the following term

$$\begin{aligned}
\delta W_2 &= M \cdot \sum_{j=1}^3 \frac{\partial \Omega}{\partial \dot{\mathbf{q}}_j} \delta \dot{\mathbf{q}}_j \\
&= M \cdot (R^T \delta R)
\end{aligned} \tag{2-24}$$

The variations in energy and the virtual work can be substituted into Equation 2-15.

Equation 2-26 is a function of variations on manifolds, where δR is a variation on $SO(3)$ and δq is a variation on \mathbb{S}^2 . The so called infinitesimal variations required to solve this equation are described as [14, 15]

$$\begin{aligned}
\delta q &= \xi \times q \in T_q \mathbb{S}^2, \text{ where } \xi \in \mathbb{R}^3, \xi \cdot q = 0 \\
\delta \dot{q} &= \\
\delta R &= R\hat{\eta} \in T_R SO(3), \text{ where } \eta \in \mathbb{R}^3, \hat{\eta} \in \mathfrak{so}(3) \\
\delta \dot{R} &= \\
\delta \hat{\Omega} &=
\end{aligned} \tag{2-25}$$

Substituting the variations in energy and the variations in

$$\begin{aligned}
\delta S &= \int_{t_1}^{t_2} (\delta W_1 + \delta W_2 + \delta \mathcal{T} - \delta \mathcal{U}) dt \\
&= \\
&=
\end{aligned} \tag{2-26}$$

The **QR** attitude kinematics equation is given by

$$\begin{aligned}
\dot{x}_L &= \\
(m_Q + m_L)(\dot{v}_L + ge_3) &= \\
\dot{q} &= \\
m_Q L \dot{\omega} &= \\
\dot{R} &= R\hat{\Omega} \\
J\dot{\Omega} + \Omega \times J\Omega &=
\end{aligned} \tag{2-27}$$

2-4 Classical Modeling

This section describes the derivation of the model by using classical modeling techniques.
NEEDED??

When assuming small angle maneuvers, *Euler-angles* can be used to locally parameterize the orientation of the body-fixed reference coordinate frame with respect to the inertial reference coordinate frame. Simple linear controllers are often based on a linearized dynamical model, applying this small angles assumption.

From Newton's law follows

$$\begin{aligned}\dot{x}_Q &= v_Q \\ m_Q \dot{v}_Q &= f R e_3 - m_Q g e_3 - T q \\ \dot{x}_L &= v_L \\ m_L \dot{v}_L &= -m_L g e_3 + T q\end{aligned}\tag{2-28}$$

Because the Euler-Angles are used, a function is required that maps a vector of the Z-X-Y Euler angles to its rotation matrix $R \in SO(3)$, which is denoted as [16]

$$R_{312}(\phi, \theta, \psi) = \begin{bmatrix} c_\psi c_\theta - s_\phi s_\psi s_\theta & -c_\phi s_\psi & c_\psi s_\theta + c_\theta s_\phi s_\psi \\ c_\theta s_\psi + c_\psi s_\phi s_\theta & c_\phi c_\psi & s_\psi s_\theta - c_\psi c_\theta s_\phi \\ -c_\phi s_\theta & s_\phi & c_\phi c_\theta \end{bmatrix}\tag{2-29}$$

The Z-X-Y Euler angles to model the rotation can be seen in Figure 2-7. The first rotation by yaw angle ψ is around the z-axis of $\{\mathcal{I}\}$. Next is the rotation by roll angle ϕ , and the last rotation is by pitch angle θ .

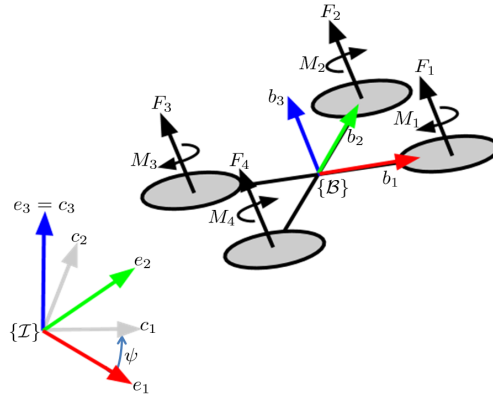


Figure 2-7: Quadrotor-Load model representation

The unit vector q from the QR to the load is represented in $\{\mathcal{B}\}$. Define ϕ_L as the yaw-rotation of the load around the z-axis of $\{\mathcal{B}\}$ and θ_L as the angle between the cable and the z-axis of $\{\mathcal{B}\}$, see Figure 2-8.

$$q = \begin{bmatrix} s_{\theta_L} c_{\phi_L} \\ s_{\theta_L} s_{\phi_L} \\ c_{\theta_L} \end{bmatrix}\tag{2-30}$$



Figure 2-8

Differentiating Equation (2-10) and (2-30) gives

$$\ddot{x}_L = \ddot{x}_Q - \ddot{q}L$$

$$\ddot{q} = \begin{bmatrix} \ddot{\theta}_L c_{\theta_L} c_{\phi_L} - \ddot{\phi}_L s_{\theta_L} s_{\phi_L} - \dot{\phi}_L^2 s_{\theta_L} c_{\phi_L} - \dot{\theta}_L^2 s_{\theta_L} c_{\phi_L} - 2\dot{\theta}_L \dot{\phi}_L c_{\theta_L} s_{\phi_L} \\ \ddot{\theta}_L c_{\theta_L} s_{\phi_L} + \ddot{\phi}_L s_{\theta_L} c_{\phi_L} - \dot{\phi}_L^2 s_{\theta_L} s_{\phi_L} - \dot{\theta}_L^2 s_{\theta_L} s_{\phi_L} + 2\dot{\theta}_L \dot{\phi}_L c_{\theta_L} c_{\phi_L} \\ -\ddot{\theta}_L s_{\theta_L} - \ddot{\phi}_L c_{\theta_L} \end{bmatrix} \quad (2-31)$$

$$\ddot{x}_Q = \frac{1}{m_Q} (f(c_\psi s_\theta + c_\theta s_\phi s_\psi) - T s_{\theta_L} c_{\psi_L})$$

$$\ddot{y}_Q = \frac{1}{m_Q} (f(s_\psi s_\theta - c_\psi c_\theta s_\phi) - T s_{\theta_L} s_{\psi_L}) \quad (2-32)$$

$$\ddot{z}_Q = \frac{1}{m_Q} (f(c_\phi c_\theta) - T c_{\theta_L}) - g$$

$$\ddot{\psi} = \ddot{\tau}_\psi \quad (2-33)$$

$$\ddot{\theta} = \ddot{\tau}_\theta \quad (2-34)$$

$$\ddot{\phi} = \ddot{\tau}_\phi \quad (2-35)$$

2-5 Stability Analysis

Lyapunov Analysis on SO3 x R3 and S2 x R3 Closed-loop full-attitude dynamics evolve on the non- Euclidean manifold SO3 x R3, while closed-loop re- duced-attitude dynamics evolve on the non-Euclidean mani- fold S2 x R3. Since these manifolds are locally Euclidean, local stability properties of a closed-loop equilibrium solution can be assessed using standard Lyapunov methods. In ad- dition, the LaSalle invariance result and related Lyapunov results apply to closed-loop vector fields defined on these manifolds. However, since the manifolds SO132 and S2 are compact, the radial unboundedness assumption cannot be satisfied; consequently, global asymptotic stability cannot fol- low from a Lyapunov analysis on Euclidean spaces [40], and therefore must be analyzed in alternative ways [19]–[23]. [8, p.43]

2-6 Summary

Compact, unambiguous, globally defined,

Pro/Cons of Classical Modeling Techniques vs Geometric Modeling

Linearized model/State Space model vs. Geometric modeling

Geometric Mechanics/Lie Groups/Lie Algebra is used in order to represent the dynamics of the system onto the nonlinear configuration manifold $SE(3)$

Advantage of this method is

Enables to model on

That type of control is discussed in the next chapter

Geometric Control Design

[14, 17]

Geometric Control Theory explores the application of differential geometric techniques to systems control. The objective is to express both the dynamics and its control inputs on manifolds instead of on local charts. Geometric control theory is the study of how the geometry of the state space influences controls problems. This includes local properties like curvature, and global properties like the number of ‘holes’ in the space (sphere vs doughnut).

Geometric Control is based on a coordinate-free representation of the dynamics, where the equations of motion are compact, unambiguous and singularity free. Globally defined (no singularities!). Therefore, one can build almost globally attractive controllers

Attitude control systems naturally evolve on non-linear configurations such as \mathbb{S}^2 and $SO(3)$. Tracking control system can be developed on $SO(3)$, therefore it avoids singularities of Euler-Angles.

Global nonlinear dynamics of various classes of closed loop attitude control systems have been studied in recent years [?]. In contrast to hybrid control systems [18], **complicated reachability set analysis is not required** to guarantee safe switching between different flight modes, as the region of attraction for each flight mode covers the configuration space almost globally.

3-1 Backstepping Control

A backstepping approach, or cascade control, is a Lyapunov based technique to design the control of nonlinear dynamical systems, while ensuring Lyapunov stability. The principle is to create a cascaded structure by starting with a stable system as a base, then ”stepping back” from the base to add a control loop around it that stabilizes the added subsystem. This is repeated until the the final external control is reached. The control law is designed by using states as virtual control signals. Each loop outputs a virtual command signal, denoted by subscript c , for the inner loop to track in order to control the outer loop.



Figure 3-1: Backstepping Control representation of the QR

A backstepping control approach is common for QRs [?] and can be seen in Figure 3-1. The lowest level has the highest bandwidth and is in control of the rotor rotational speeds. The next level controls the QR attitude, and the top level controls the QR position.

Because the QR has only four actuators, it is not possible to control all DOFs of the QR-Load system. Therefore, different flight modes are specified in which parts of the DOFs are controlled. The same backstepping approach allows different flight modes that are defined as follows

- QR Attitude Controlled Mode
 - Track a desired QR attitude command $R_d(t)$ and a heading direction $b_{1_d}(t)$
- Load Attitude Controlled Mode
 - Track a desired load attitude command $q_d(t)$
- Load Position Controlled Mode
 - Track a desired load position $x_{L,d}(t)$



Figure 3-2: Backstepping Control representation of the QR-Load system

3-2 Configuration Errors

Before the controllers are described, the configuration functions are defined as in [14]. These functions describe the error on the manifolds that describe the configuration spaces for the QR attitude $\in SO(3)$ and the load attitude $\in \mathbb{S}^2$.

Define errors associated with the attitude dynamics of the QR.

The QR attitude error function on $SO(3)$ is chosen to be [3]

$$\Psi_R(R, R_d) = \frac{1}{2} \text{tr} [I - R_d^T R] \quad (3-1)$$

Ψ_R is locally positive-definite about $R_d^T R = I$ within the region where the rotation angle between R and R_d is less than 180° [14].

The derivative of Equation 3-1 is given by

$$\mathbf{D}_R \Psi(R, R_d) \cdot R \hat{\eta} = \frac{1}{2} (R_d^T R - R^T R_d)^\vee \cdot \eta \quad (3-2)$$

where the *vee map* $^\vee : \mathfrak{so}(3) \rightarrow \mathbb{R}^3$ is the inverse of the *hat map* defined in Section 2-2.

The tracking error functions on $TSO(3)$, the tangent space of $SO(3)$, are defined as

$$e_R = \frac{1}{2} (R_d^T R - R^T R_d)^\vee \quad (3-3)$$

The tangent vectors \dot{R} and \dot{R}_d cannot be compared directly, since they do lie in the same space. They each are defined in their own tangent spaces, denoted by $\dot{R} \in T_R SO(3)$ and $\dot{R}_d \in T_{R_d} SO(3)$. In order to define an error function, \dot{R}_d is transformed into a vector on $T_R SO(3)$. This can be done by an mathematical object that is called a *transport map*, it connects tangent spaces at different points.

Considering the definitions of Equations 2-4 and 2-5, \dot{R}_d can be compared with \dot{R} , by defining a connection as follows

$$\begin{aligned} \dot{R} - \dot{R}_d(R_d^T R) &= R \hat{\Omega} - R_d \hat{\Omega}_d(R_d^T R) \\ &= R(\Omega)^\wedge - (R R^T) R_d \hat{\Omega}_d R_d^T R \\ &= R(\Omega)^\wedge - R(R^T R_d \Omega_d)^\wedge \\ &= R(\Omega - R^T R_d \Omega_d)^\wedge \end{aligned} \quad (3-4)$$

With the use of Equation 2-5 and 2-6

$$\begin{aligned} \frac{d}{dt}(R_d^T R) &= (R_d^T \dot{R}) + (\dot{R}_d^T R) \\ &= (R_d^T (R \hat{\Omega})) + ((R_d \hat{\Omega}_d)^T R) \\ &= R_d^T R(\Omega)^\wedge - (\hat{\Omega}_d R_d^T) R \\ &= R_d^T R(\Omega)^\wedge - (R_d^T R R^T R_d) \hat{\Omega}_d R_d^T R \\ &= R_d^T R(\Omega - R^T R_d \Omega_d)^\wedge \\ &= (R_d^T R) \hat{e}_\Omega \end{aligned} \quad (3-5)$$

$$\hat{e}_\Omega = (\Omega - R^T R_d \Omega_d)^\wedge \quad (3-6)$$

The tracking error for the angular velocity of the rotation matrix $(R_d^T R)$ expressed in $\{\mathcal{B}\}$ follows from Equation 3-5 and is defined as

$$e_\Omega = \Omega - R^T R_d \Omega_d \quad (3-7)$$

The error function on \mathbb{S}^2 is chosen to be

$$\Psi_q = 1 - q_d^T q \quad (3-8)$$

The tracking error functions on the tangent space of \mathbb{S}^2 , denoted by $T\mathbb{S}^2$ are defined as

$$e_q = \hat{q}^2 q_d \quad (3-9)$$

$$e_{\dot{q}} = \dot{q} - (q_d \times \dot{q}_d) \times q \quad (3-10)$$

The tracking errors for position and velocity are defined as

$$e_x = x - x_d \quad (3-11)$$

$$e_v = v - v_d \quad (3-12)$$

where $v_d = \dot{x}_d$ and $x_d(t) \in \mathbb{R}^3$ is a smooth desired load position.

3-3 Quadrotor Attitude Tracking

QR Attitude Controlled Mode is designed to control the attitude of the QR by tracking a desired QR attitude command $R_d(t)$ and a heading direction $b_{1_d}(t)$. The controller is shown in Figure 3-3.



Figure 3-3: Quadrotor Attitude Controller

The calculation of the moment consists of a proportional term, a derivative term and a canceling term, and is defined as follows

$$M = \frac{1}{\epsilon^2} k_R e_R - \frac{1}{\epsilon} k_\Omega e_\Omega + \Omega \times J\Omega - J(\hat{\Omega} R^T R_d \Omega_d - R^T R_d \dot{\Omega}_d) \quad (3-13)$$

for any positive constants k_R, k_Ω , and $0 < \epsilon < 1$. Where ϵ is a parameter to enable rapid exponential convergence of the attitude error functions.

It is proven in [3] that the zero equilibrium of the closed loop tracking error $(e_R, e_\Omega) = (0, 0)$ is exponentially stable, if the initial conditions satisfy

$$\Psi_R(R(0), R_d(0)) < 2 \quad (3-14)$$

$$\|e_\Omega(0)\|^2 < \frac{2}{\lambda_M(J)} \frac{k_R}{\epsilon^2} (2 - \Psi_R(R(0), R_d(0))) \quad (3-15)$$

where $\lambda_M(\cdot)$ denotes the maximum eigenvalue.

Furthermore, there exist constants $\alpha_R, \beta_R > 0$ such that

$$\Psi_R(R(t), R_d(t)) \leq \min \left\{ 2, \alpha_R e^{-\beta_R t} \right\} \quad (3-16)$$

In [3] the derivation of a stability analysis of the controller is presented.

3-4 Load Attitude Tracking

Tracks load attitude reference. Outputs attitude reference to attitude controller.

How is the controller built.

Dependent of what values? How to choose parameters.



Figure 3-4

$$R = \quad (3-17)$$

It is proven in [15] that the zero equilibrium of the closed loop tracking error $(e_q, e_{\dot{q}}, e_R, e_{\Omega}) = (0, 0, 0, 0)$ is exponentially stable, if the initial conditions satisfy

$$\Psi_q(q(0), q_d(0)) < 2 \quad (3-18)$$

$$\|e_{\dot{q}}(0)\|^2 < \frac{2}{m_Q L} k_R (2 - \Psi_q(q(0), q_d(0))) \quad (3-19)$$

The domain of attraction is defined by Equations 3-14, 3-15, 3-18 and 3-19.

Furthermore, there exist constants $\alpha_q, \beta_q > 0$ such that

$$\Psi_q(q(t), q_d(t)) \leq \min \left\{ 2, \alpha_q e^{-\beta_q t} \right\} \quad (3-20)$$

3-5 Load Position Tracking

Tracks load position reference. Outputs load attitude reference.

$$q = \quad (3-21)$$



Figure 3-5

It is proven in [15] that the zero equilibrium of the closed loop tracking error $(e_x, e_v, e_q, e_{\dot{q}}, e_R, e_\Omega) = (0, 0, 0, 0, 0, 0)$ is exponentially stable, if the initial conditions satisfy

$$\Psi_q(q(0), q_c(0)) < \psi_1 < 1 \quad (3-22)$$

$$\|e_x(0)\|^2 < e_{x_{max}} \quad (3-23)$$

where $e_{x_{max}}$ and ψ_1 are fixed constants.

The domain of attraction is defined by Equations 3-14, 3-15, 3-22 and the following equation

$$\|e_{\dot{q}}(0)\|^2 < \frac{2}{m_Q L} k_q (\psi_1 - \Psi_q(q(0), q_d(0))) \quad (3-24)$$

Furthermore, there exist constants $\alpha_q, \beta_q > 0$ such that

$$\Psi_q(q(t), q_d(t)) \leq \min \left\{ 2, \alpha_q e^{-\beta_q t} \right\} \quad (3-25)$$

3-6 Parameter- and State Estimation

How to choose parameters and how to select gains for errors

How to estimate states?

What parameters must be

Refer to Lyapunov stability analysis [14]

3-7 Summary

What is Geometric Control?

Why Geometric Control?

Control design will be based on Nonlinear Geometric Control

The proposed control system is robust to switching conditions since each flight mode has almost global stability properties, and it is straightforward to design a complex maneuver of a QR. [19] Where are the Error functions based on?

Form bridge between Geometric Control and Hybrid Control

Why Hybrid Control?

Parameter Estimation can be done by

State Estimation can be done by

Drawback: assumes all states to be known

Model based. What if analytical model is not accurate?

Experiments and Results

In Section 4-1 the experimental setup is explained. The chosen model- and controller parameters are presented.

The experiments that are used are explained and discussed in Section 4-2, of which the results are presented and discussed in Section 4-2.

A conclusion is made based on the obtained results in Section 4-3.

4-1 Setup

Model parameters The simulations are developed using Matlab and Simulink, using the system parameters found in Table 4-1.

Parameter	Value	Description
m_Q	4.34 kg	Quadrotor Mass
m_L	0.1 kg	Load Mass
l	0.315 m	Arm length from QR CoM to rotor
L	0.7 m	Cable Length
I_{xx}	0.0820 kgm^2	Quadrotor Inertia about x-axis
I_{yy}	0.0845 kgm^2	Quadrotor Inertia about y-axis
I_{zz}	0.1377 kgm^2	Quadrotor Inertia about z-axis
d		Drag Constant
b		Thrust Constant
c_{τ_f}		Constant

Table 4-1: Modeling Parameters

LQR Control A Linear Quadratic Regulator (LQR) controller is used to compare the performance of the nonlinear geometric controller. LQR control uses an algorithm to obtain

a state-feedback controller, minimizing a cost function depending on the states and weight factors.

An LQR design is shown in Figure 4-1



Figure 4-1: LQR control design

LQR control is based on a small angle assumption. Therefore, a traditional modeling method may represent the rotation matrix with a local coordinate system, for example with an Euler Angle parameterization. A continuous time linearized model of the system used in this controller is represented in the following form

$$\dot{\mathbf{x}} = A\mathbf{x} + Bu \quad (4-1)$$

$$y = C\mathbf{x} + Du \quad (4-2)$$

where

$$\mathbf{x} = \begin{bmatrix} \mathbf{q} \\ \dot{\mathbf{q}} \end{bmatrix} \quad (4-3)$$

$$\mathbf{q} = [x \ y \ z \ \phi \ \theta \ \psi \ \phi_L \ \theta_L]^T \quad (4-4)$$

$$\dot{\mathbf{q}} = [\dot{x} \ \dot{y} \ \dot{z} \ \dot{\phi} \ \dot{\theta} \ \dot{\psi} \ \dot{\phi}_L \ \dot{\theta}_L]^T \quad (4-5)$$

$$u = [f \ M_\phi \ M_\theta \ M_\psi]^T \quad (4-6)$$

The derivation of A, B, C, D, K can be found in Section A-2.

Using `Matlab` command `lqr(A,B,Q,R)`, an optimal gain matrix K is calculated, such that the state-feedback law $u = -K\mathbf{x}$ minimizes the quadratic cost function defined as

$$J(u) = \int_0^\infty (\mathbf{x}^T Q \mathbf{x} + u^T R u) dt \quad (4-7)$$

The tuning parameters of the LQR controller are chosen as follows

$$\begin{aligned} Q &= \text{diag}(1010100, 111, 11, 111, 111, 11) \\ R &= \text{diag}(0.0441, 561.561, 56) \end{aligned} \quad (4-8)$$

where Q and R denote weight matrices that penalize the states and inputs in the cost function. where the state \mathbf{x} and input u are defined as

$$\mathbf{x} = \begin{bmatrix} \mathbf{q} \\ \dot{\mathbf{q}} \end{bmatrix} \quad (4-9)$$

$$\mathbf{q} = [x \ y \ z \ \phi \ \theta \ \psi \ \theta_L \ \psi_L]^T \quad (4-10)$$

$$\dot{\mathbf{q}} = [\dot{x} \ \dot{y} \ \dot{z} \ \dot{\phi} \ \dot{\theta} \ \dot{\psi} \ \dot{\theta}_L \ \dot{\psi}_L]^T \quad (4-11)$$

$$u = [f \ M_\phi \ M_\theta \ M_\psi]^T \quad (4-12)$$

Geometric Control The chosen controller gains in Equations 3-13,3-17,3-21 can be found in Table 4-2.

Gain	Value
k_R	
k_Ω	
k_q	
k_ω	
k_x	
k_v	

Table 4-2: Controller Gains

4-1-1 Command Filtering

Implementation of the backstepping approach also increases the order of the states. Thus, a consequence of backstepping control is that inner control loops become a function of the commanded signals and their higher derivatives, generated by an outer loop. Instead of analytic differentiation of these terms, which can be tedious and require high computational costs, these values can be obtained with the use of a Command Filter, which is explained in more detail in [20].

Basically, the command signal is pre-filtered by a low pass filter with the following state space representation

$$\dot{x}_1 = x_2 \quad (4-13)$$

$$\dot{x}_2 = x_3 \quad (4-14)$$

$$\dot{x}_3 = -(2\zeta\omega_{n2} + \omega_{n1})x_3 - (2\zeta\omega_{n1}\omega_{n2} + \omega_{n2}^2)x_2 - (\omega_{n1}\omega_{n2}^2)(x_1 - x_c^o) \quad (4-15)$$

where $x_1 = x_c$, $x_2 = \dot{x}_c$ and $x_3 = \ddot{x}_c$.

The transfer function of the original commanded input signal X_c^o and the filtered output X_c has the form

$$\frac{X_c(s)}{X_c^o(s)} = H(s) = \frac{\omega_{n1}}{s + \omega_{n1}} \cdot \frac{\omega_{n2}^2}{s^2 + 2\zeta\omega_{n2}s + \omega_{n2}^2} \quad (4-16)$$

Where ζ is the damping ratio and ω_n the undamped natural frequency. See Figure 4-2 and A-1.

This command filter is implemented to compute $\dot{R}_c, \ddot{R}_c, \dot{q}_c, \ddot{q}_c$.

The load attitude controller generates a commanded QR attitude R_c and its derivative \dot{R}_c . In the same fashion, the load position controller generates a commanded load attitude q_c and its derivative \dot{q}_c .

The controllers are functions of these commanded signals and their derivatives. Instead of analytic differentiation of these signals, they are obtained by integration by applying a third order low pass filter to the original signals R_c^o and q_c^o . The state space implementation of this third order filter is [21]



Figure 4-2: Representation of the command filter

$$\frac{x_c}{x_c^o} = \frac{\omega_{n1}}{s + \omega_{n1}} \cdot \frac{\omega_{n2}^2}{s^2 + 2\zeta\omega_{n2}s + \omega_{n2}^2} \quad (4-17)$$

$$\Rightarrow x_c''' = -(2\zeta\omega_{n2} + \omega_{n1})x_c'' - (2\zeta\omega_{n1}\omega_{n2} + \omega_{n2}^2)x_c' - (\omega_{n1}\omega_{n2}^2)(x_c - x_c^o) \quad (4-18)$$

4-2 Experiments

LQR is an optimal control strategy and will be used to compare its result to a Nonlinear Geometric Controller.

$x_d(t)$ is required to be smooth for the Geometric Control. Trajectories are generated by hand, however it is possible to compute these with trajectory generating algorithms too.

4-2-1 Performance Criteria

Performance that can be evaluated for different cases can be specified by the following

- Step Response
 - Settling time (if swing minimization is important)
 - Rising time (important if time critical)
 - Overshoot (if max swing is critical)
 - Steady state error / swing of load (if accuracy is important)
 - Max load angle
- Disturbance Rejection
- Trajectory tracking
 - Can we minimize time, while minimizing position error (All Cases)
 - Minimum position error (All Cases)
 - Maximum amplitude/frequency of wave with respect to stability (Case B)
- Computational Effort (?)

4-2-2 Case A

In this case a smooth step-like trajectory is generated to transport the load from the starting position along one direction in order to reach the final position.

It will show if the system is fast enough to track the position.

From point A to point B The fast

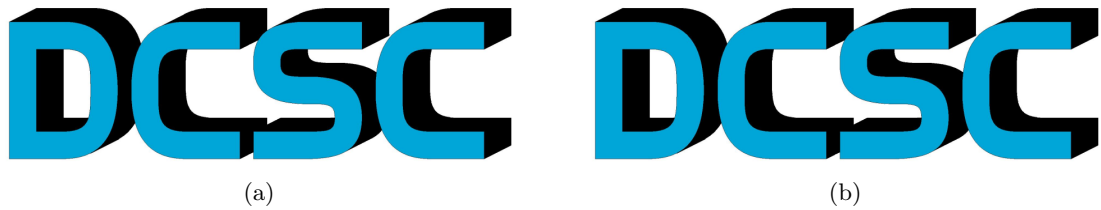


Figure 4-3: Desired Load Position Case A

4-2-3 Case B

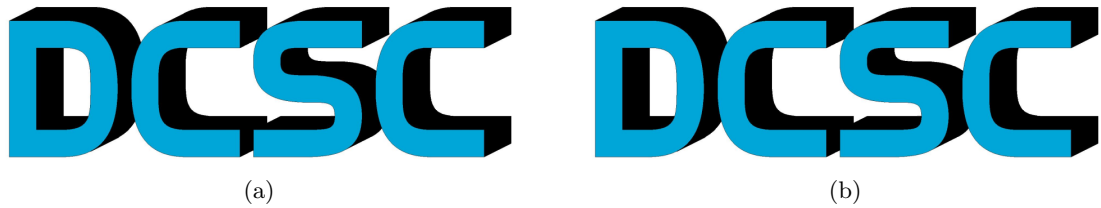


Figure 4-4: Desired Load Position Case B

4-2-4 Case C

In this case a trajectory is generated to test multiple disciplines. The trajectory has the shape of a sine wave that varies in amplitude in the direction of the x-axis, while moving along the y-axis and going up and down in height. Different velocities are required to track the trajectory. While tracking the right QR attitude to reach these velocities, it can be expected to be harder for the controller to also maintain the desired height.

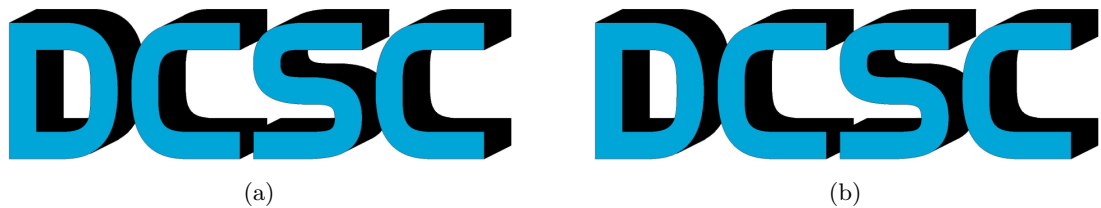


Figure 4-5: Desired Load Position Case C

4-3 Results

4-3-1 Case A

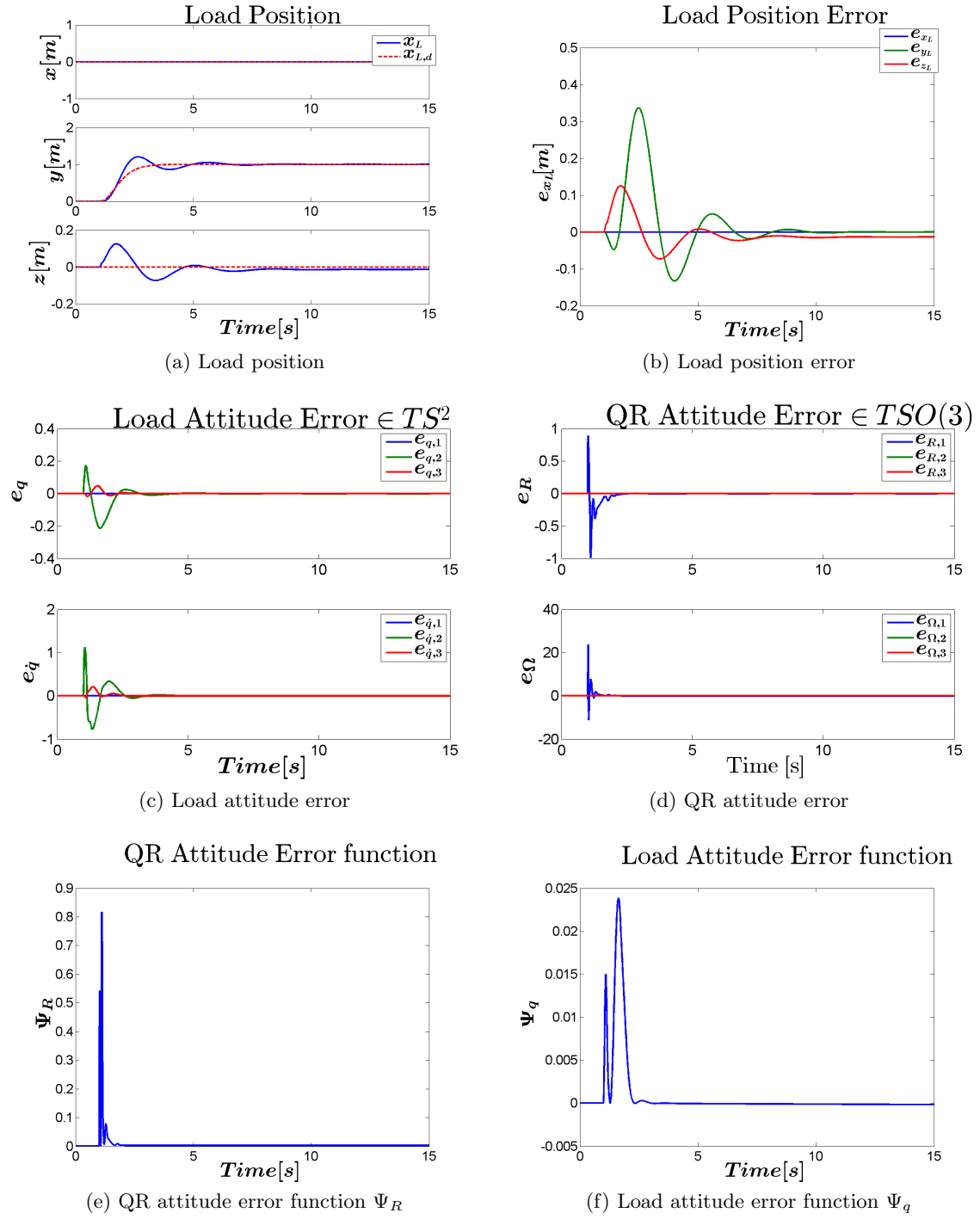


Figure 4-6: Results Nonlinear Geometric Control Case A

4-3-2 Case B

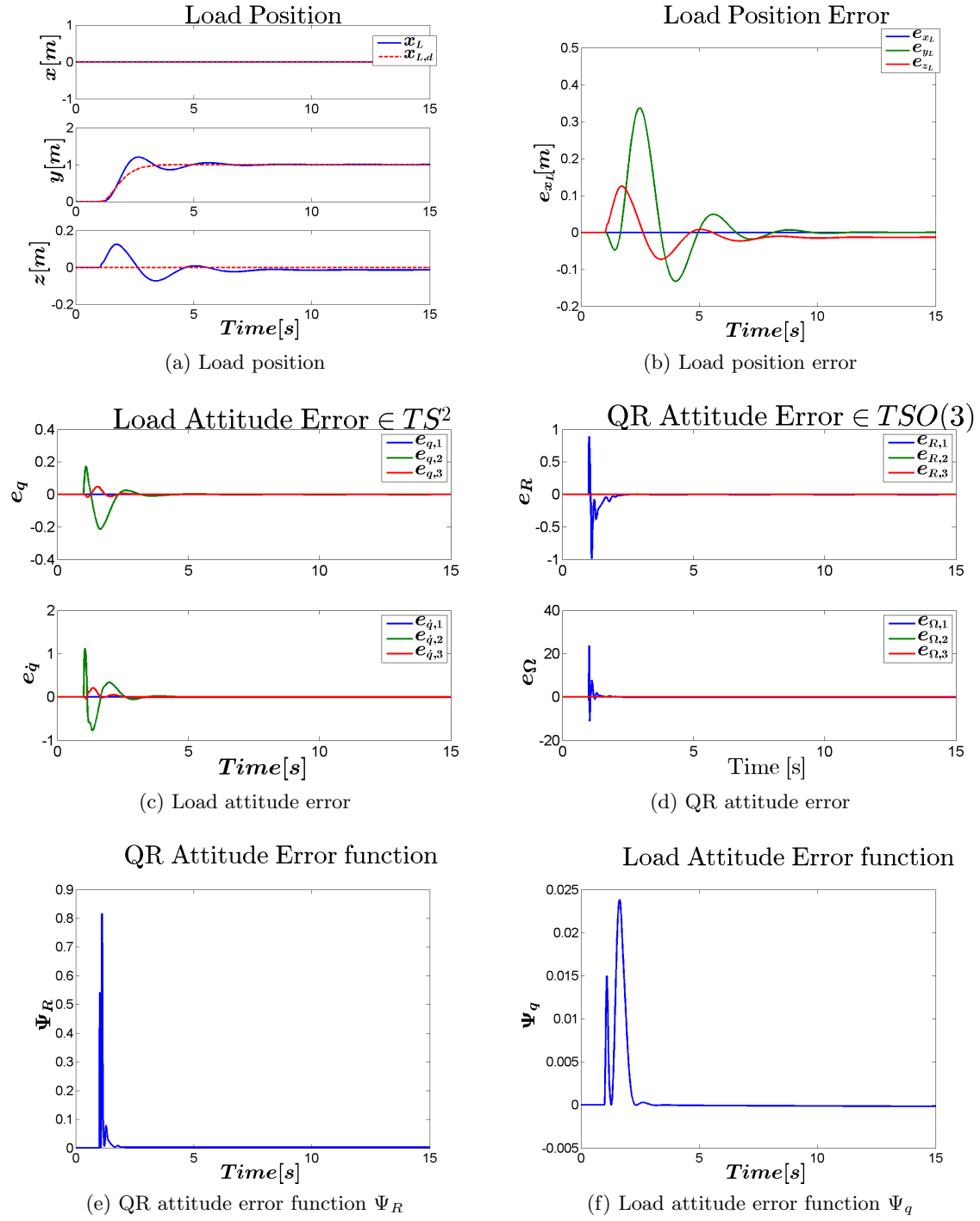


Figure 4-7: Results Nonlinear Geometric Control Case B

4-3-3 Case C

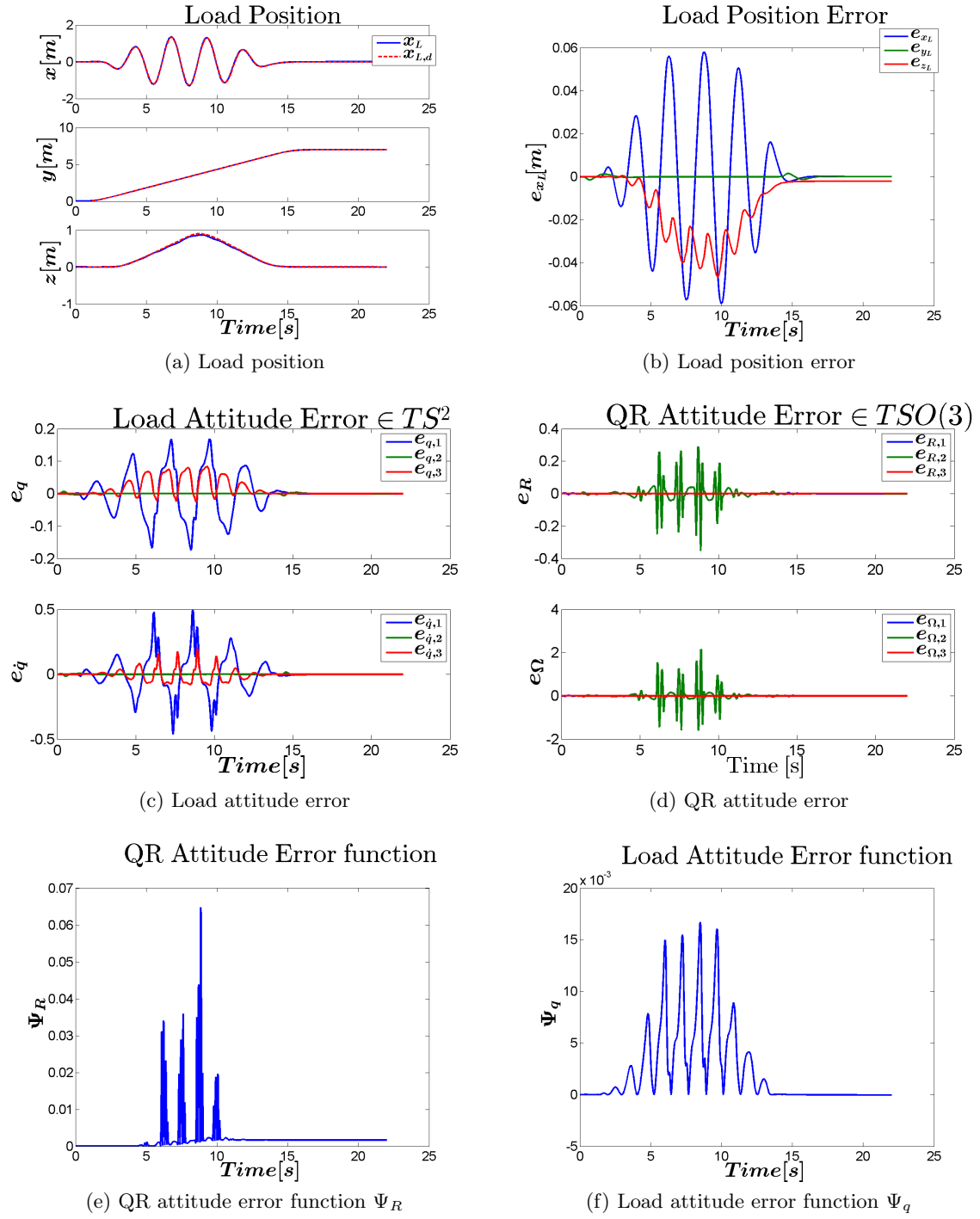


Figure 4-8: Results Nonlinear Geometric Control Case C

4-4 Conclusion

Conclusions and Future Work

5-1 Summary and Conclusions

The report starts with an introduction to the subject. The aim is described and the motivation for this research is given.

In the following chapter A short introduction of the concepts of differential geometry

Next, the nonlinear geometric control design is explained. Backstepping is explained

Experiments are defined. Testing the nonlinear Geometric Controller To compare with a common linear controller, [LQR](#) control is used to compare Results are,

The conclusions we could extract from the experiments is that

5-2 Recommendations for Future Work

5-2-1 Investigate Implementation

Lack of time: no implementation possible. In order to realize this, one needs to investigate the subjects described in this section.

Can in be implemented in terms of computational power? Can this be run on on-board processor? Problem is already partly simplified by command filter. Quantification and comparison between implemented [MPC](#) and Geometric Control.

Model identification and validation. Now it is an estimation and/or taken from other literature.

How to deal with noise?

The control is designed assuming continuous-time control. In a real-time application the control of the [QR](#) is limited to its bandwidth.

5-2-2 Modeling Constraints

There are several techniques to handle input saturation, the most popular ones are anti-windup techniques. Back-calculation is such a method for PID to activate the integrator, is this possible for NL control?

[4] includes uncertainties in the translational dynamics and rotational dynamics. Out of the scope, might be interesting.

5-2-3 Hybrid Modeling

Switching between several flight modes yields autonomous acrobatic maneuvers. Robust to switching conditions ***why?

[7]

5-2-4 Trajectory Generation

Minimum Snap Trajectory Generation

Trajectory can be generated by solving a **QP!** via minimum snap generation.

Problem in smaller 4-D space instead of 12-D, with help of differential flatness. Explain differential flatness and its usefulness.

Is able to include constraints in **QP!**.

[22]

Obstacle avoidance

Appendix A

Appendix

A-1 Derivation of Equations of motion

A-1-1 Load Dynamics

Let x_{CM} denote the position of the center of mass of the combined Quadrotor-Load system, expressed in $\{\mathcal{I}\}$. Which can be found by

$$\begin{aligned} m_Q(x_Q - x_{CM}) + m_L(x_L - x_{CM}) &= 0 \\ (m_Q + m_L)x_{CM} &= m_Q x_Q + m_L x_L \end{aligned} \tag{A-1}$$

Applying the laws of motion to (A-1) and inserting (2-10) gives the

$$\begin{aligned} (m_Q + m_L)\ddot{x}_{CM} &= fRe_3 - (m_Q + m_L)ge_3 \\ (m_Q + m_L)(\ddot{x}_L + ge_3) &= fRe_3 + m_Q L\ddot{q} \end{aligned} \tag{A-2}$$

A-2 LQR controller

A-2-1 Modeling

The linearized model is written into a first order ODE of the form

$$\dot{\mathbf{x}} = A\mathbf{x} + Bu \tag{A-3}$$

$$y = C\mathbf{x} + Du \tag{A-4}$$

with the following state- and input vectors

$$\begin{aligned} \mathbf{x} &= \begin{bmatrix} \mathbf{q} \\ \dot{\mathbf{q}} \end{bmatrix} \\ \mathbf{q} &= [x \ y \ z \ \phi \ \theta \ \psi \ \phi_L \ \theta_L]^T \\ \dot{\mathbf{q}} &= [\dot{x} \ \dot{y} \ \dot{z} \ \dot{\phi} \ \dot{\theta} \ \dot{\psi} \ \dot{\phi}_L \ \dot{\theta}_L]^T \\ u &= [f \ M_\phi \ M_\theta \ M_\psi]^T \end{aligned} \tag{A-5}$$

The model is linearized about the hovering flight mode. All translational and rotational velocities are zero during hover. The positional states and the yaw angle do not affect the dynamics, and are set equal to zero. A thrust input $u_1 = g(mQ + mL)$ is required to maintain hover, and all other control inputs are set equal to zero. The states and inputs in the equations of motion are substituted by an initial condition and a perturbation

$$\dot{\mathbf{x}} \rightarrow \dot{\mathbf{x}}_0 + \delta\dot{\mathbf{x}}, \quad \mathbf{x} \rightarrow \mathbf{x}_0 + \delta\mathbf{x}, \quad u \rightarrow u_0 + \delta u \quad (\text{A-6})$$

$$\begin{aligned} \mathbf{x}(0) &= \mathbf{0} \\ u(0) &= [g(mQ + mL) \quad 0 \quad 0 \quad 0]^T \end{aligned} \quad (\text{A-7})$$

The linearized equations of motion are rearranged into Equation A-8 and substituted in Equation A-3.

$$[\text{content...}] \begin{bmatrix} \delta\ddot{x} \\ \delta\ddot{y} \\ \delta\ddot{z} \\ \delta\ddot{\phi} \\ \delta\ddot{\theta} \\ \delta\ddot{\psi} \\ \delta\ddot{\phi}_L \\ \delta\ddot{\theta}_L \end{bmatrix} + [\text{content...}] \begin{bmatrix} \delta x \\ \delta y \\ \delta z \\ \delta\phi \\ \delta\theta \\ \delta\psi \\ \delta\phi_L \\ \delta\theta_L \end{bmatrix} = [\text{content...}] \begin{bmatrix} \delta u_1 \\ \delta u_2 \\ \delta u_3 \\ \delta u_4 \end{bmatrix} \quad (\text{A-8})$$

1	LQRA =															
	Columns 1 through 8															
	0	0	0	0	0	0	0	0	0	0	0	0	0	0	0	0
6	0	0	0	0	0	0	0	0	0	0	0	0	0	0	0	0
	0	0	0	0	0	0	0	0	0	0	0	0	0	0	0	0
	0	0	0	0	0	0	0	0	0	0	0	0	0	0	0	0
	0	0	0	0	0	0	0	0	0	0	0	0	0	0	0	0
11	0	0	0	0	0	0	0	0	0	0	0	0	0	0	0	0
	0	0	0	0	0	0	0	0	0	0	0	0	0	0	0	0
	0	0	0	9.7008	0	0	0	0	0.1092	0	0	0	0	0	0	0
	0	0	0	0	-9.9217	0	0	0	0	0	0.1117	0	0	0	0	0
	0	0	0	0	0	0	0	0	0	0	0	0	0	0	0	0
16	0	0	0	0	0	0	0	0	0	0	0	0	0	0	0	0
	0	0	0	0	0	0	0	0	0	0	0	0	0	0	0	0
	0	0	0	6.9291	0	0	0	0	-6.9291	0	0	0	0	0	0	0
	0	0	0	0	7.0870	0	0	0	0	0	-7.0870	0	0	0	0	0
21	Columns 9 through 16															
	1.0000	0	0	0	0	0	0	0	0	0	0	0	0	0	0	0
	0	1.0000	0	0	0	0	0	0	0	0	0	0	0	0	0	0
26	0	0	1.0000	0	0	0	0	0	0	0	0	0	0	0	0	0
	0	0	0	1.0000	0	0	0	0	0	0	0	0	0	0	0	0
	0	0	0	0	1.0000	0	0	0	0	0	0	0	0	0	0	0

	0	0	0	0	0	1.0000	0	0
	0	0	0	0	0	0	1.0000	0
31	0	0	0	0	0	0	0	1.0000
	0	0	0	0	0	0	0	0
	0	0	0	0	0	0	0	0
	0	0	0	0	0	0	0	0
	0	0	0	0	0	0	0	0
	0	0	0	0	0	0	0	0
36	0	0	0	0	0	0	0	0
	0	0	0	0	0	0	0	0
	0	0	0	0	0	0	0	0
	0	0	0	0	0	0	0	0

1	LQRB =							
	0	0	0	0				
	0	0	0	0				
	0	0	0	0				
6	0	0	0	0				
	0	0	0	0				
	0	0	0	0				
	0	0	0	0				
	0	0	0	0				
11	0	-0.1591	0	0				
	0	0	-0.1627	0				
	0.2252	0	0	0	0			
	0	12.1951	0	0				
	0	0	11.8343	0				
16	0	0	0	7.2622				
	0	10.0905	0	0				
	0	0	10.3203	0				

Matlab command `lqr(A,B,Q,R)` generates the following gain matrix K

	K =							
2	Columns 1 through 8							
	-0.0000	-0.0000	47.6731	0.0000	-0.0000	0.0000	-0.0000	0.0000
	3.1623	0.0000	-0.0000	7.5117	0.0000	-0.0000	2.6683	-0.0000
7	-0.0000	-3.1623	-0.0000	0.0000	7.4605	0.0000	-0.0000	2.5448
	0.0000	-0.0000	0.0000	-0.0000	0.0000	1.0000	0.0000	0.0000
	Columns 9 through 16							
12	-0.0000	-0.0000	21.1202	0.0000	0.0000	0.0000	-0.0000	-0.0000
	2.7501	0.0000	-0.0000	1.4827	0.0000	0.0000	0.4376	-0.0000
	-0.0000	-2.7296	0.0000	0.0000	1.4631	0.0000	-0.0000	0.3949
	0.0000	-0.0000	0.0000	0.0000	-0.0000	1.1293	-0.0000	0.0000

A-2-2 Controller

$$A = [\text{content...}] \quad (\text{A-9})$$

$$B = [content...] \quad (A-10)$$

$$C = [content...] \quad (A-11)$$

$$\dot{\mathbf{x}} = \mathbf{f}(\mathbf{x}, \mathbf{u}) \quad (A-12)$$

A-3 Figures



Figure A-1: Simulink Command Filter

A-4 MATLAB code

$$Testequation \quad (A-13)$$

A-4-1 A MatlabListing

```
%  
% Comment  
%  
n=10;  
5 for i=1:n  
    disp('Ok');  
end
```

Bibliography

- [1] M. Bangura and R. Mahony, “Real-time model predictive control for quadrotors,” in *IFAC Proceedings Volumes (IFAC-PapersOnline)*, vol. 19, pp. 11773–11780, 2014.
- [2] R. P. K. Jain and T. Keviczky, “MSc Thesis: Transportation of Cable Suspended Load using Unmanned Aerial Vehicles: A Real-time Model Predictive Control approach,” 2015.
- [3] T. Lee, M. Leok, and N. H. McClamroch, “Geometric Tracking Control of a Quadrotor UAV on $SE(3)$,” *49th IEEE Conference on Decision and Control*, no. 3, pp. 5420–5425, 2010.
- [4] F. Goodarzi, D. Lee, and T. Lee, “Geometric nonlinear PID control of a quadrotor UAV on $SE(3)$,” *Control Conference (ECC), 2013 European*, pp. 3845–3850, 2013.
- [5] K. Sreenath, N. Michael, and V. Kumar, “Trajectory generation and control of a quadrotor with a cable-suspended load - A differentially-flat hybrid system,” in *Proceedings - IEEE International Conference on Robotics and Automation*, pp. 4888–4895, 2013.
- [6] K. Sreenath, T. Lee, and V. Kumar, “Geometric control and differential flatness of a quadrotor UAV with a cable-suspended load,” in *Proceedings of the IEEE Conference on Decision and Control*, pp. 2269–2274, 2013.
- [7] S. Tang, “Aggressive Maneuvering of a Quadrotor with a Cable-Suspended Payload,” tech. rep., University of Pennsylvania Philadelphia, Pennsylvania, 2014.
- [8] N. Chaturvedi, “Attitude control,” *IEEE Control Systems*, vol. 31, no. 3, pp. 30–51, 2011.
- [9] R. M. Murray, Z. Li, and S. S. Sastry, *A Mathematical Introduction to Robotic Manipulation*, vol. 29. 1994.
- [10] T. Lee, *Computational Geometric Mechanics and Control of Rigid Bodies*. PhD thesis, The University of Michigan, 2008.

- [11] T. L. T. Lee, N. McClamroch, and M. Leok, "A lie group variational integrator for the attitude dynamics of a rigid body with applications to the 3D pendulum," *Proceedings of 2005 IEEE Conference on Control Applications, 2005. CCA 2005.*, pp. 962–967, 2005.
- [12] T. Lee, M. Leok, and N. H. McClamroch, "Lagrangian mechanics and variational integrators on two-spheres," *International Journal for Numerical Methods in Engineering*, vol. 79, no. 9, pp. 1147–1174, 2009.
- [13] T. Lee, M. Leok, and N. H. McClamroch, "Stable Manifolds of Saddle Points for Pendulum Dynamics on S^2 and $SO(3)$," p. 9, 2011.
- [14] F. Bullo and A. D. Lewis, *Geometric control of mechanical systems: modeling, analysis, and design for simple mechanical control systems*. Springer, 2005.
- [15] K. Sreenath, Taeyoung Lee, and V. Kumar, "Geometric control and differential flatness of a quadrotor UAV with a cable-suspended load," in *52nd IEEE Conference on Decision and Control*, pp. 2269–2274, IEEE, dec 2013.
- [16] R. Mahony, V. Kumar, and P. Corke, "Multirotor Aerial Vehicles: Modeling, Estimation, and Control of Quadrotor," *IEEE Robotics & Automation Magazine*, vol. 19, no. 3, pp. 20–32, 2012.
- [17] V. Jurdjevic, *Geometric Control Theory*. Cambridge: Cambridge University Press, 1997.
- [18] J. H. Gillula, H. Huang, M. P. Vitus, and C. J. Tomlin, "Design of guaranteed safe maneuvers using reachable sets: Autonomous quadrotor aerobatics in theory and practice," in *Proceedings - IEEE International Conference on Robotics and Automation*, pp. 1649–1654, 2010.
- [19] T. Lee, M. Leok, and N. McClamroch, "Control of complex maneuvers for a quadrotor UAV using geometric methods on $SE(3)$," *arXiv*, 2010.
- [20] J. A. Farrell, M. Polycarpou, M. Sharma, and W. Dong, "Command Filtered Backstepping," pp. 1923–1928, 2008.
- [21] V. Djapic, J. Farrell, and W. Dong, "Land vehicle control using a command filtered backstepping approach," *Proceedings of the American Control Conference*, pp. 2461–2466, 2008.
- [22] D. Mellinger and V. Kumar, "Minimum snap trajectory generation and control for quadrotors," in *Proceedings - IEEE International Conference on Robotics and Automation*, pp. 2520–2525, 2011.

Bibliography

- [1] M. Bangura and R. Mahony, “Real-time model predictive control for quadrotors,” in *IFAC Proceedings Volumes (IFAC-PapersOnline)*, vol. 19, pp. 11773–11780, 2014.
- [2] R. P. K. Jain and T. Keviczky, “MSc Thesis: Transportation of Cable Suspended Load using Unmanned Aerial Vehicles: A Real-time Model Predictive Control approach,” 2015.
- [3] T. Lee, M. Leok, and N. H. McClamroch, “Geometric Tracking Control of a Quadrotor UAV on $SE(3)$,” *49th IEEE Conference on Decision and Control*, no. 3, pp. 5420–5425, 2010.
- [4] F. Goodarzi, D. Lee, and T. Lee, “Geometric nonlinear PID control of a quadrotor UAV on $SE(3)$,” *Control Conference (ECC), 2013 European*, pp. 3845–3850, 2013.
- [5] K. Sreenath, N. Michael, and V. Kumar, “Trajectory generation and control of a quadrotor with a cable-suspended load - A differentially-flat hybrid system,” in *Proceedings - IEEE International Conference on Robotics and Automation*, pp. 4888–4895, 2013.
- [6] K. Sreenath, T. Lee, and V. Kumar, “Geometric control and differential flatness of a quadrotor UAV with a cable-suspended load,” in *Proceedings of the IEEE Conference on Decision and Control*, pp. 2269–2274, 2013.
- [7] S. Tang, “Aggressive Maneuvering of a Quadrotor with a Cable-Suspended Payload,” tech. rep., University of Pennsylvania Philadelphia, Pennsylvania, 2014.
- [8] N. Chaturvedi, “Attitude control,” *IEEE Control Systems*, vol. 31, no. 3, pp. 30–51, 2011.
- [9] R. M. Murray, Z. Li, and S. S. Sastry, *A Mathematical Introduction to Robotic Manipulation*, vol. 29. 1994.
- [10] T. Lee, *Computational Geometric Mechanics and Control of Rigid Bodies*. PhD thesis, The University of Michigan, 2008.

- [11] T. L. T. Lee, N. McClamroch, and M. Leok, "A lie group variational integrator for the attitude dynamics of a rigid body with applications to the 3D pendulum," *Proceedings of 2005 IEEE Conference on Control Applications, 2005. CCA 2005.*, pp. 962–967, 2005.
- [12] T. Lee, M. Leok, and N. H. McClamroch, "Lagrangian mechanics and variational integrators on two-spheres," *International Journal for Numerical Methods in Engineering*, vol. 79, no. 9, pp. 1147–1174, 2009.
- [13] T. Lee, M. Leok, and N. H. McClamroch, "Stable Manifolds of Saddle Points for Pendulum Dynamics on S^2 and $SO(3)$," p. 9, 2011.
- [14] F. Bullo and A. D. Lewis, *Geometric control of mechanical systems: modeling, analysis, and design for simple mechanical control systems*. Springer, 2005.
- [15] K. Sreenath, Taeyoung Lee, and V. Kumar, "Geometric control and differential flatness of a quadrotor UAV with a cable-suspended load," in *52nd IEEE Conference on Decision and Control*, pp. 2269–2274, IEEE, dec 2013.
- [16] R. Mahony, V. Kumar, and P. Corke, "Multirotor Aerial Vehicles: Modeling, Estimation, and Control of Quadrotor," *IEEE Robotics & Automation Magazine*, vol. 19, no. 3, pp. 20–32, 2012.
- [17] V. Jurdjevic, *Geometric Control Theory*. Cambridge: Cambridge University Press, 1997.
- [18] J. H. Gillula, H. Huang, M. P. Vitus, and C. J. Tomlin, "Design of guaranteed safe maneuvers using reachable sets: Autonomous quadrotor aerobatics in theory and practice," in *Proceedings - IEEE International Conference on Robotics and Automation*, pp. 1649–1654, 2010.
- [19] T. Lee, M. Leok, and N. McClamroch, "Control of complex maneuvers for a quadrotor UAV using geometric methods on $SE(3)$," *arXiv*, 2010.
- [20] J. A. Farrell, M. Polycarpou, M. Sharma, and W. Dong, "Command Filtered Backstepping," pp. 1923–1928, 2008.
- [21] V. Djapic, J. Farrell, and W. Dong, "Land vehicle control using a command filtered backstepping approach," *Proceedings of the American Control Conference*, pp. 2461–2466, 2008.
- [22] D. Mellinger and V. Kumar, "Minimum snap trajectory generation and control for quadrotors," in *Proceedings - IEEE International Conference on Robotics and Automation*, pp. 2520–2525, 2011.

Nomenclature

ω_i Angular velocity of rotor i around its axis, $i = \{1, 2, 3, 4\}$

$\tau_{drag,i}$ Drag moment generated by each propellor

$\{\mathbf{b}_1, \mathbf{b}_2, \mathbf{b}_3\}$ Unit vectors along the axes of $\{\mathcal{B}\}$

$\{\mathbf{c}_1, \mathbf{c}_2, \mathbf{c}_3\}$ Unit vectors along the axes of $\{\mathcal{C}\}$

$\{\mathbf{e}_1, \mathbf{e}_2, \mathbf{e}_3\}$ Unit vectors along the axes of $\{\mathcal{I}\}$

$\{\mathcal{B}\}$ Body Frame

$\{\mathcal{C}\}$ Intermediary Frame

$\{\mathcal{I}\}$ Inertial World Frame

b Thrust factor

d Drag factor

L Length of the cable

q Unit vector from Quadrotor to Load

x_L Position of the of the Quadrotor CM

x_Q Position of the of the Quadrotor CM

x_{CM} Position CM of Quadrotor-Load system

Acronyms

QR	Quadrotor
UAV	Unmanned Aerial Vehicle
CoM	Center of Mass
DOF	Degree of Freedom
PID controller	Proportional-Integral-Derivative Controller
MPC	Model Predictive Control
Nonlinear MPC	Nonlinear Model Predictive Control
LQR	Linear Quadratic Regulator
QP	Quadratic Programming